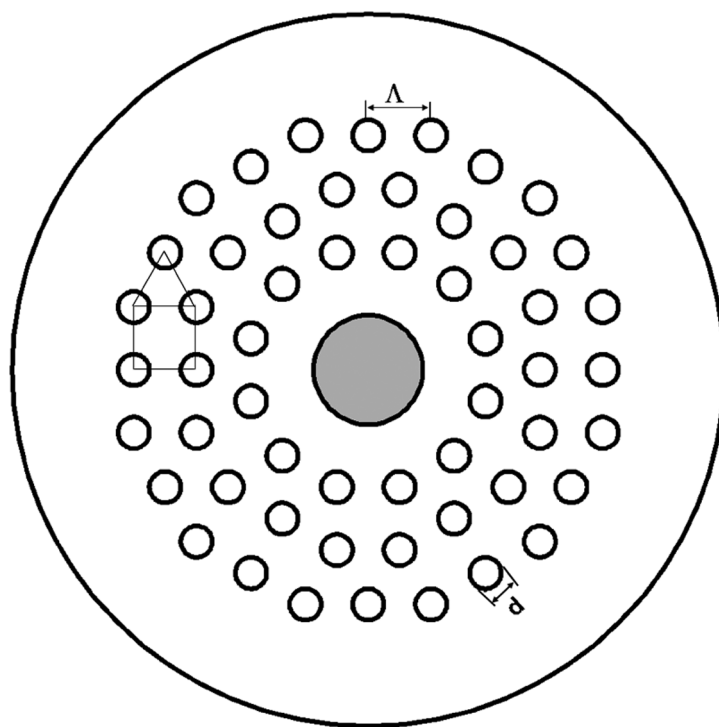


# Large Pitch Photonic Quasi-Crystal Fiber Amplifier

Volume 4, Number 3, June 2012

S. Sivabalan, Member, IEEE  
J. P. Raina



DOI: 10.1109/JPHOT.2012.2201147  
1943-0655/\$31.00 ©2012 IEEE

# Large Pitch Photonic Quasi-Crystal Fiber Amplifier

S. Sivabalan,<sup>1</sup> *Member, IEEE*, and J. P. Raina<sup>2</sup>

<sup>1</sup>School of Electrical Engineering, VIT University, Vellore 632014, India

<sup>2</sup>Centre for Nanotechnology Research, VIT University, Vellore 632014, India

DOI: 10.1109/JPHOT.2012.2201147  
1943-0655/\$31.00 ©2012 IEEE

Manuscript received May 3, 2012; revised May 17, 2012; accepted May 17, 2012. Date of publication May 24, 2012; date of current version May 31, 2012. Corresponding author: S. Sivaraj (e-mail: s.sivab@gmail.com).

**Abstract:** We design an ytterbium-doped large pitch photonic quasi-crystal fiber (PQF) for amplifying high-energy ultrashort laser pulses. The proposed fiber exhibits unique properties such as very large mode area ( $4660 \mu\text{m}^2$ ), less attenuation (0.42 dB/km), high overlapping factor (0.55 for the fundamental mode), and low bending loss. These properties help amplify with high-average power ultrashort pulses with less distortion and high efficiency. To meet these requirements, we design a fiber with optimum gain filtering as well as loss filtering. From the numerical simulation of the analytical model, we confirm that the large pitch PQF plays an indispensable role in amplifying high-energy ultrashort pulses.

**Index Terms:** Photonic quasi-crystal fibers (PQFs), fiber amplifier, chirped pulse amplification, large mode area fiber, ultrashort pulse amplifier.

## 1. Introduction

Chirped pulse fiber amplification is one of the most successful techniques used for amplifying ultrashort pulses. The development of chirped pulse fiber amplifier (CPFA) has reached a stage of amplifying pulse energy as high as 2.2 mJ [1] which is comparable to that from bulk type solid state amplifiers. Large mode area (LMA) of the fiber is the reason behind the high power handling capacity in CPFA. It reduces the nonlinearity and increases the damage threshold of the fiber. For further scaling of power in CPFA system, the mode area of the doped fiber is increased with the single mode property being maintained. The single mode behavior in LMA fiber amplifier is one of the important topics of interest since it decides the beam properties namely beam stability and beam focusability in high power regime [2]. In very large mode area (VLMA) fibers, maintaining single mode behavior has always been a challenging task. Increasing the mode area in fibers leads to increase in higher order modes (HOMs), which, in turn, may result in highly multimode propagation. The popular method of removing HOMs has been by means of coiling of fiber [3]. However, this method turns futile with the VLMA fibers owing to their larger diameter. Some of the techniques known for larger diameter fibers are gain guiding while index antiguiding [4], resonant coupling of HOMs [5] and modified spatial dopant profiles [6]. In conventional fiber, although VLMA is implemented successfully, the design flexibility becomes difficult for improving other properties like reducing bending loss, larger dispersion, extended single mode cutoff, etc. [7]. VLMA in fibers has been achieved with the holey structures in the cladding known as the photonic crystal fiber (PCF) [8]. It has emerged as an alternative for the conventional fiber owing to its enhanced LMA properties [9].

PCF possesses a high degree of freedom in meeting the desired properties such as endlessly single mode nature, high or low dispersion, LMA and high birefringence, which cannot be achieved with conventional fibers [10]. LMA PCF has a capability for scaling the mode area of the fiber with minimum bending loss. There are various designs in practice for achieving LMA in PCF. The most noted fiber designs which are currently used in CPFA systems for producing high-energy pulses are leakage channel fiber and rod type PCF [8], [11]. These fibers are also known as large pitch fibers since their pitch is greater by ten times the operating wavelength. In these fibers, single-modedness is achieved by two methods. The first one is by loss filtering that involves differential loss for fundamental and HOMs [12]. The second method deals with gain filtering i.e., the fundamental mode (FM) is promoted with both high gain and low loss compared to HOMs [7]. This is done by keeping the doped area lesser than the fiber core area and this results in high gain for the FM and very low gain for HOMs. Both the hitherto mentioned fiber types have hexagonal holey structures which exhibit large attenuation as well as high bending loss and experience the degradation of the beam quality in the event of increasing the diameter of the fiber.

In this paper, we propose a photonic quasi-crystal fiber (PQF) for increasing the mode area with minimum bending loss, low attenuation and high overlap factor. PQFs have unique properties such as ultraflattened dispersion [13], larger cutoff ratio for endlessly single mode operation [14], two photonic band gaps with low loss guidance [15] and a very large dispersion in addition to the LMA characteristics [16]. Photonic quasi-crystal cladding results in unusual characteristics which are not noticeable in photonic crystal cladding. Over the years, photonic quasi-crystals have been playing an indispensable role for enhancing the light extraction in III-Nitrides based light-emitting diodes (LEDs) [17], [18] and Organic LEDs [19]. In addition, they also help increase the light trapping capability in thin film silicon solar cell [20].

To the best of our knowledge, this is the first proposal for large pitch PQF which has the best features of both conventional fiber and PCF, namely, the circular core profile and holey cladding structure. Here, we introduce both loss filtering and gain filtering onto the same fiber for the enhancement of amplifier properties. Further, we prove using a suitable analytical model that the proposed fiber has the capability of producing high-average power. This fiber may turn out to be an appropriate choice for realizing a high-energy or high-average power amplifier for ultrashort pulses.

## 2. Theoretical Basis

### 2.1. Method of Analysis

We use fully vectorial finite element method (FEM) for solving Maxwell's equations that govern the field distribution in the cross section of fiber structure. Here, the region which is being analyzed is surrounded by a perfectly matched layer (PML) absorbing boundary condition for calculating loss parameters of the fiber. The PCF cross section is divided into subdomains with quadratic triangular elements. The output of the simulation results in real and imaginary parts of the effective mode index  $n_{\text{eff}}$ . The field distribution of the fiber modes will also be obtained for each mode. By including PML, the resultant fully vectorial wave equation is derived from the Maxwell's equations [21]

$$\nabla \times \left( [\mu]_{\text{PML}}^{-1} \nabla \times \vec{E} \right) - k_0^2 [\varepsilon]_{\text{PML}} \vec{E} = 0 \quad (1)$$

where  $k_0$  is the free space wavenumber, and  $\vec{E}$  is the electric field vector. The parameters  $[\mu]_{\text{PML}}$  and  $[\varepsilon]_{\text{PML}}$  are the permittivity and permeability tensors of the PML regions, respectively.

### 2.2. Amplifier Model

In this section, we adopt the well-known analytical model for the ytterbium-doped fiber amplifier to study the effect of overlap factor of pump  $\Gamma_p$  and signal  $\Gamma_s$  over the average signal output power.

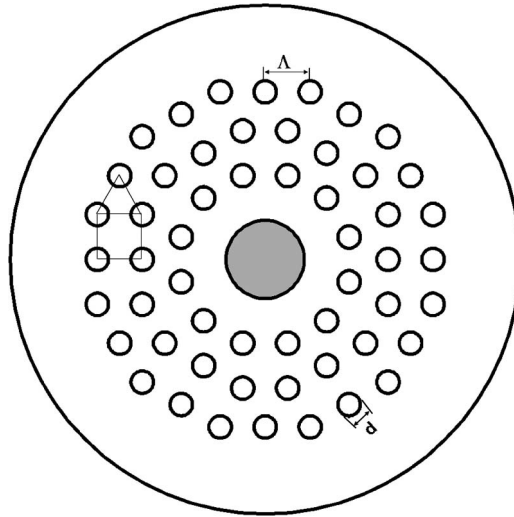


Fig. 1. Schematic cross section of PQF. White circles denote the air holes.  $\Delta$  is the distance between the adjacent air holes,  $d$  is the diameter of the air holes and core is index depressed (gray).

The spatio-temporal evolutions of the pump  $P_p(z)$  and of the signal  $P_s(z)$  are given by, respectively [22]–[24]

$$\frac{dP_p}{dz} = \Gamma_p [\sigma_e(\lambda_p) N_2(z) - \sigma_a(\lambda_p) N_1(z)] N_{tot} P_p(z) \quad (2)$$

$$\frac{dP_s}{dz} = \Gamma_s [\sigma_e(\lambda_s) N_2(z) - \sigma_a(\lambda_s) N_1(z)] N_{tot} P_p(z). \quad (3)$$

Here,  $N_1(z)$  and  $N_2(z)$  are the population density for lower and upper levels, respectively. The parameters  $\sigma_a(\lambda_p)$  and  $\sigma_e(\lambda_s)$  represent the absorption and emission cross sections of pump and signal, respectively.

### 3. Design of the Large Pitch PQF

The proposed fiber is designed to encompass the desired characteristics such as LMA, good beam quality, minimum bending loss, high overlapping factor, low attenuation loss for FM and high loss for HOMs. The cross section of six-fold symmetry PQF with large pitch is shown in Fig. 1. The core is formed by 7 missing holes i.e., removing the center and the immediate hexagonal ring holes. Thus, this takes the diameter of the core as  $100 \mu\text{m}$ . The doped diameter of the fiber is varied from 25 to  $75 \mu\text{m}$  and it is optimized to provide high gain for the FM when compared to that of HOMs. The cladding of the fiber is formed by the combination of square and triangular unit cells. It is known that the number of rings in the cladding decides the confinement loss of the fiber. Usually more numbers of rings are preferred for low confinement loss. But, this ultimately ends up in complicated fabrication process. To overcome this challenge, we propose a novel design with the circular shape core and three rings in the cladding. This new design offers low confinement loss in addition to the ease of fabrication process.

The pitch of the fiber is fixed as  $30 \mu\text{m}$  based on the diameter of the fiber. The relative air hole size  $d/(\Delta)$  is varied from 0.15 to 0.5 and it is optimized according to minimum attenuation and bending loss with high overlapping factor. The refractive index of the ytterbium-doped core is maintained as 1.45 throughout this work to retrieve the refractive index value of the fused silica [2]. Another designing criterion is the index depression which is defined as the refractive index difference between silica and the doped core i.e.,  $\Delta n = n_{\text{silica}} - n_{\text{doped}}$ . This index depression is introduced for enhancing the mode field diameter and the preferential gain of the FM [2]. Further, the index depression increases the mode discrimination capability of the fiber which in turn results

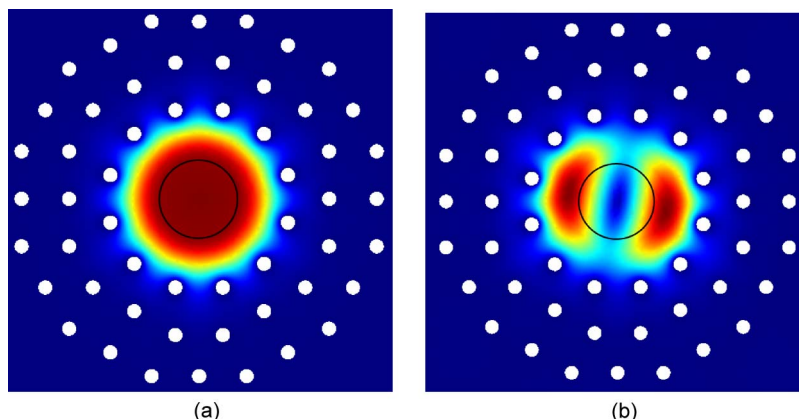


Fig. 2. (a) Field distribution of  $LP_{01}$  mode and (b) First order field distribution with index depression of  $4 \times 10^{-5}$ .

in mode filtering [12]. The core of the proposed PQF is highly circular when compared to hexagonal shape of the conventional PCF and former one does improve the various properties of large pitch fiber.

## 4. Characteristics of the Proposed PQF

### 4.1. Modal Characteristics

Having discussed the appropriate theoretical background and designing aspects of large pitch PQF, now, we delineate on the different characteristics of the same. The diameter of the doped region is chosen to be  $50 \mu\text{m}$ . The electric field distribution of the fundamental mode and the first HOM is shown in Fig. 2. This analysis is carried out at  $1.06 \mu\text{m}$  wavelength. The fundamental mode field in PQF is highly circular, like in the case of the standard single mode fiber, due to the circular cladding as depicted in Fig. 2(a). This circular field distribution is not possible in the conventional PCF since, for larger values of  $d/\Lambda$ , the horizontal and vertically polarized light components do not exhibit rotational symmetry due to the deviation in circular shape of the mode by hexagonal structure [25]. The refractive index of the doped region is reduced by  $4 \times 10^{-5}$ . The index depression process shifts the first order mode which is shown in Fig. 2(b) and eventually, it is out of the doped region. Here, field distribution due to HOMs need not be analyzed as their fields lie outside the doped core. The depressed index doping simultaneously enhances the mode area and reduces the confinement of light at the center of the core. This leads to decrease in nonlinearity of the fiber.

### 4.2. Mode Loss Analysis

The fundamental mode loss is an important parameter of an amplifier in deciding the efficiency. In this section, we compute the loss of the fundamental mode for various values of  $d/\Lambda$  and then compare this with that of conventional PCF. Fig. 3(a) represents the FM loss of PQF for various values of  $d/\Lambda$ . From this figure, it is seen that the loss is constant for wavelengths ranging from  $1.0$  to  $1.1 \mu\text{m}$  and for  $d/\Lambda$ , from  $0.15$  to  $0.5$ . Here, the pitch value is roughly 30 times greater than the wavelength and hence, the loss remains constant for a desired range of input wavelength. The lowest loss occurs, when  $d/\Lambda = 0.5$ , due to the increase of air hole size. Fig. 3(b) illustrates the confinement loss of  $LP_{01}$  mode of the PQF as well as conventional PCF of triangular hole arrangement. The values of  $\Lambda$  and  $(d/\Lambda)$  are fixed as  $30 \mu\text{m}$  and  $0.3$ , respectively, for both the fibers. The confinement loss for the PQF is found to be ten times lesser than that of the conventional PCF. This is due to the highly circular nature of the cladding which eventually enhances the light confinement.

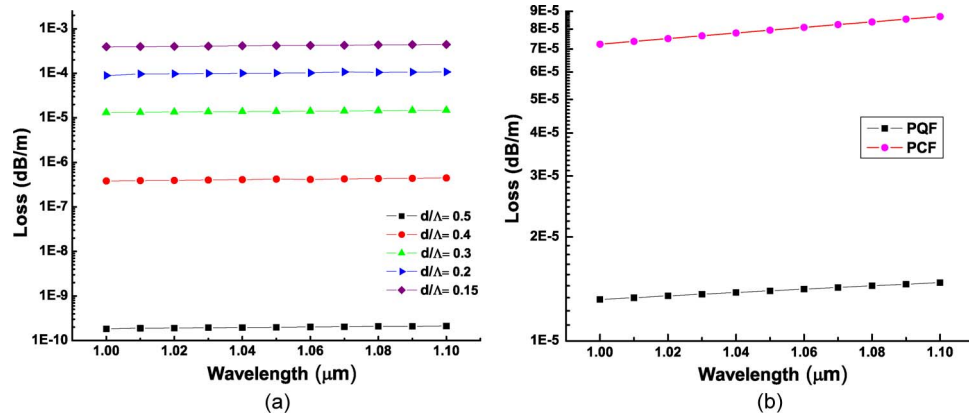


Fig. 3. (a) FM loss for different values of  $d/\Lambda$  (b) FM loss for PQF and PCF for  $d/\Lambda = 0.3$ .

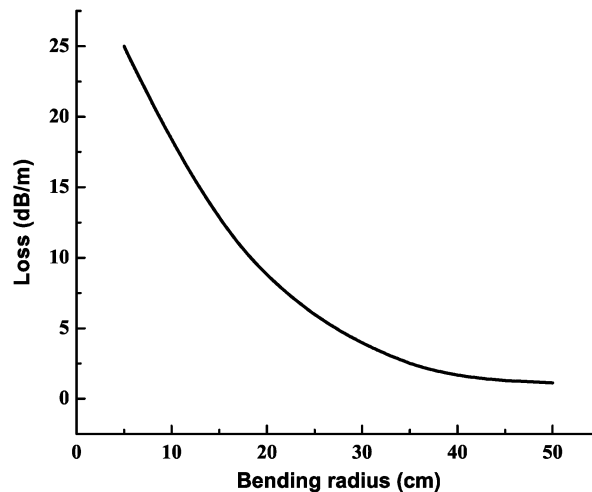


Fig. 4. Bending loss of the fundamental mode of PQF as a function of bending radius.

#### 4.3. Bending Loss Characteristics

Next, we study an important parameter called bending loss which indeed decides the compactness of the amplifier system. Here, we determine the bending loss for the PQF by replacing the refractive index profiles of the fiber with an equivalent refractive index profile of a bent fiber computed by an equivalent straight waveguide formulation [21]. In this case, we assign,  $\Lambda = 30 \mu\text{m}$  and  $d = 9 \mu\text{m}$  and keep the doped diameter as  $50 \mu\text{m}$  and study the bending along the  $x$ -direction. Fig. 4 shows the bending loss characteristics of PQF for various values of bending radii. Here, it can be noted that the loss is almost constant up to 30 cm and increases exponentially for lesser bending radius. Further, we emphasize that the loss for the PQF is less when compared to other large pitch fibers with more inner cladding rings. The reason for the low bending loss is that the circular cladding structure of PQF prevents the leakage of field into the cladding.

#### 4.4. Influence of Index Depression Over the Effective Area and Overlap Factor

The index depression is an important technique for enhancing mode area. Further, this increases the loss for HOMs. However, the increase of index depression reduces the overlap factor due to the less confinement of FM at the center of the core. Therefore, an optimum value of index depression has to be determined by optimizing the effective area and overlap factor for achieving efficient

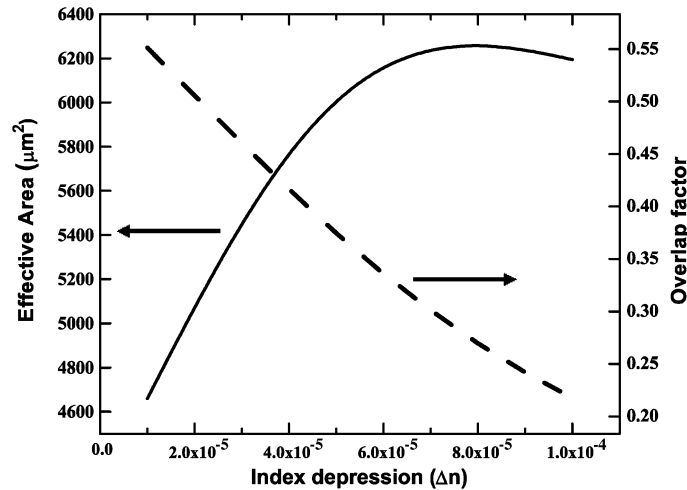


Fig. 5. Index depression versus effective area and overlap factor for the doping diameter of 50  $\mu\text{m}$ .

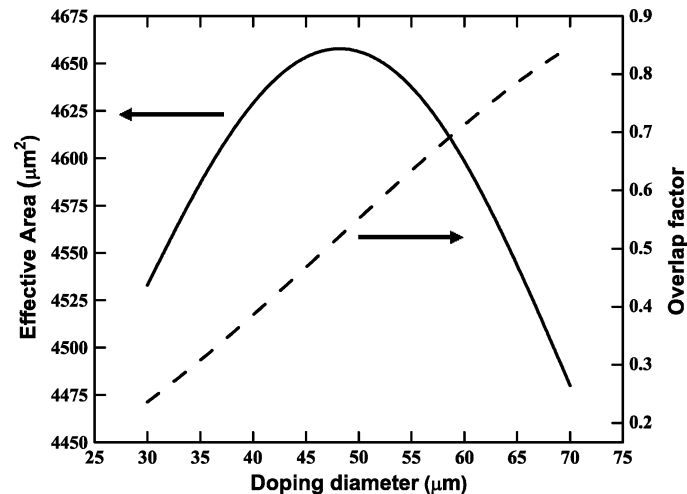


Fig. 6. Doping diameter versus effective area and overlap factor for the index depression of  $10^{-5}$ .

amplification in the system. Fig. 5 depicts the variations of effective area and overlap factor for various values of index depression. To get a maximum amplification factor (overlap factor), the index depression should be as minimum as possible. Here, for a minimum value of depression of  $10^{-5}$ , the effective area is  $4600 \mu\text{m}^2$  and the overlap factor is 0.55. It should be noted that it is practically a challenging task to obtain a minimum value of index depression in a repeatable fashion [12]. Thus we optimize the overlap factor to be 0.5 and the corresponding effective area turns to be  $4660 \mu\text{m}^2$  for best amplification with a minimum nonlinearity. It is to be noted that an index depression of  $2 \times 10^{-5}$  ensures the hither-to mentioned optimized values for effective area and overlap factor.

#### 4.5. Role of Doping Diameter Over Effective Area and Overlap Factor

The doping diameter decides the effective area and the gain of the fiber amplifier. In this section, we analyze the effect of doping diameter over the effective area and signal overlap factor of the fiber. It is necessary to optimize the doping diameter to achieve the higher effective area and to get a considerable gain with the amplifier. Fig. 6 shows the signal overlap factor for various doping

TABLE 1

Physical parameters used in the simulation

Parameter	Value
$N_{tot}$	$8.5 \times 10^{25} \text{m}^{-3}$
$\sigma_a(\lambda_p)$	$25 \times 10^{-13} \mu\text{m}^2$
$\sigma_e(\lambda_p)$	$21.7 \times 10^{-13} \mu\text{m}^2$
$\sigma_a(\lambda_s)$	$0.448 \times 10^{-13} \mu\text{m}^2$
$\sigma_e(\lambda_s)$	$2.62 \times 10^{-13} \mu\text{m}^2$
$\lambda_p$	976 nm
$\lambda_s$	1060 nm
$\tau_f$	0.8 ms
core diameter	100 $\mu\text{m}$

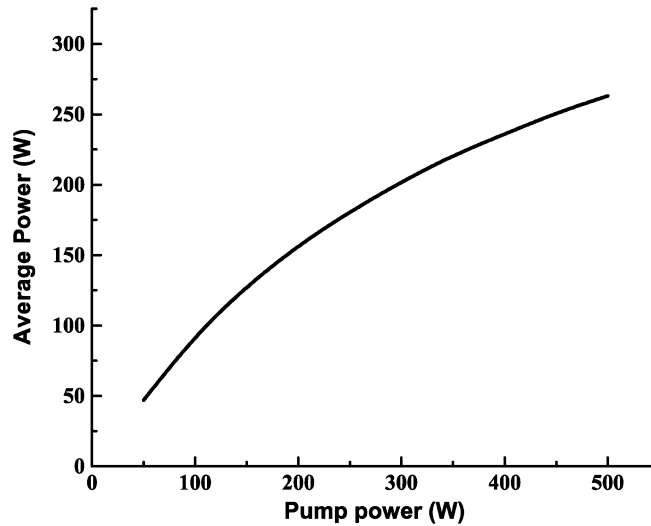


Fig. 7. Average signal output power of the amplifier versus pump power.

diameters at 1.06  $\mu\text{m}$  wavelength. We find that the overlap factor increases as the doping diameter increases. It is due to more confinement of FM within the core when the diameter of the doped core increases. The second parameter namely the effective area initially increases as doping diameter is increased and then it starts decreasing from 50  $\mu\text{m}$ . The decrement in the effective area takes place because of index depression. As and when the index depression diameter increases, the field distribution spreads out of the doping region since the refractive index of the core eventually matches with that of the value of the cladding. Therefore, the optimum diameter of the doping is 50  $\mu\text{m}$  at which effective area is 4660  $\mu\text{m}^2$  and the corresponding overlap factor is 0.55.

## 5. PQF Amplifier

This section deals with the modeling of fiber amplifier based on the proposed PQF. Here, we calculate the average power generated from the fiber amplifier using the model mentioned in Section 2.2. To study the amplification process, we solve the (2) and (3) by the well-known Runge–Kutta method. In the numerical simulation, we use the optimized value of the signal overlap factor which is 0.5. We calculate the pump overlap factor as 0.0434 which depends on the ratio of square of core radius to cladding radius. Here, the length of the fiber is chosen to be 1.2 m.

Table 1 provides the rest of the physical parameters used in the simulation [23]. Fig. 7 shows the input pump power against average output power generated by the amplifier. From the figure, it is evident that efficiency of the amplification is found to be 85% for the lower pump power while it is only about 55% for higher values of pump power. This variation in the amplification process takes place since the gain gets saturated in high power regime. Therefore, we find that the fiber amplifier performance depends mainly on the input average power, length of the fiber and overlap factors.

## 6. Conclusion

To investigate the amplification of high-energy ultrashort pulses, we have designed a large pitch PQF with remarkable properties namely, VLMA, lower bending loss, very low attenuation and high overlapping factor. The index depression has been optimized as  $2 \times 10^{-5}$  and this results in LMA with high overlap factor. From these properties, one could understand that the proposed PQF transforms into an improved version of rod type PCF wherein bending optimization is highly challenging. The numerical results pertaining to fiber amplifier corroborate that this fiber could be used in high power amplification process with an average slope efficiency of 65%. On account of the circular nature of the cladding, it is obvious that the beam quality may also be improved in high power regime.

## References

- [1] T. Eidam, J. Rothhardt, F. Stutzki, F. Jansen, S. Hadrich, H. Carstens, C. Jauregui, J. Limpert, and A. Tunnermann, "Fiber chirped-pulse amplification system emitting 3.8 GW peak power," *Opt. Exp.*, vol. 19, no. 1, pp. 255–260, Jan. 2011.
- [2] T. Eidam, S. Hadrich, F. Jansen, F. Stutzki, J. Rothhardt, H. Carstens, C. Jauregui, J. Limpert, and A. Tunnermann, "Preferential gain photonic-crystal fiber for mode stabilization at high average powers," *Opt. Exp.*, vol. 19, no. 9, pp. 8656–8661, Apr. 2011.
- [3] J. P. Kopolow, D. A. V. Klirner, and L. Goldberg, "Single-mode operation of a coiled multimode fiber amplifier," *Opt. Lett.*, vol. 25, no. 7, pp. 442–444, Jul. 2000.
- [4] V. Sudesh, T. McComb, Y. Chen, M. Bass, M. Richardson, J. Ballato, and A. E. Siegman, "Diode-pumped 200  $\mu\text{m}$  diameter core, gain-guided, index-antiguidded singlemode fiber laser," *Appl. Phys. B, Laser Opt.*, vol. 90, no. 3/4, pp. 369–372, Feb. 2008.
- [5] C. Liu, G. Chang, N. Litchinitser, D. Guertin, N. Jacobsen, K. Tankala, and A. Galvanauskas, "Chirally coupled core fibers at 1550-nm and 1064-nm for effectively single-mode core size scaling," in *Proc. Conf. Lasers Electro-Opt.*, May 6–11, 2007, pp. 1–2.
- [6] T. Bhutta, J. I. Mackenzie, D. P. Sphepherd, and R. J. Beach, "Spatial dopant profiles for transverse-mode selection in multimode waveguides," *J. Opt. Soc. Amer. B*, vol. 19, no. 7, pp. 1539–1543, Jul. 2002.
- [7] J. R. Marciante, "Gain filtering for single-spatial-mode operation of large mode area fiber amplifier," *IEEE J. Sel. Topics Quantum Electron.*, vol. 15, no. 1, pp. 30–36, Jan./Feb. 2009.
- [8] J. Limpert, O. Schmidt, J. Rothhardt, F. Röser, T. Schreiber, A. Tunnermann, S. Ermeneux, P. Yvernault, and F. Salin, "Extended single-mode photonic crystal fiber lasers," *Opt. Exp.*, vol. 14, no. 7, pp. 2715–2720, Apr. 2006.
- [9] N. A. Mortensen, M. D. Nielsen, J. R. Folkenberg, A. Petersson, and H. R. Simonsen, "Improved large-mode area endlessly single-mode photonic crystal fibers," *Opt. Lett.*, vol. 28, no. 6, pp. 393–395, Mar. 2003.
- [10] P. St. J. Russell, "Photonic crystal fibers," *J. Lightw. Technol.*, vol. 24, no. 12, pp. 4729–4749, Dec. 2006.
- [11] W. S. Wong, X. Peng, J. M. McLaughlin, and L. Dong, "Breaking the limit of maximum effective area for robust single-mode propagation in optical fibers," *Opt. Exp.*, vol. 30, no. 21, pp. 2855–2857, Nov. 2005.
- [12] F. Jansen, F. Stutzki, H. J. Otto, M. Baumgartl, C. Jauregui, J. Limpert, and A. Tunnermann, "The influence of index-depressions in core pumped Yb-doped large pitch fibers," *Opt. Exp.*, vol. 18, no. 26, pp. 26 834–26 842, Dec. 2010.
- [13] S. Kim, C. S. Kee, and J. Lee, "Novel optical properties of six-fold symmetric photonic quasicrystal fibers," *Opt. Exp.*, vol. 15, no. 20, pp. 13 221–13 226, Oct. 2007.
- [14] S. Kim and C. S. Kee, "Dispersion properties of dual-core photonic quasicrystal fiber," *Opt. Exp.*, vol. 17, no. 18, pp. 15 885–15 890, Aug. 2009.
- [15] X. Sun and D. J. J. Hu, "Air guiding with photonic quasi-crystal fiber," *IEEE Photon. Technol. Lett.*, vol. 22, no. 9, pp. 607–609, May 2010.
- [16] S. Sivabalan and J. P. Raina, "High normal dispersion and large mode area photonic quasi-crystal fiber stretcher," *IEEE Photon. Technol. Lett.*, vol. 23, no. 16, pp. 1139–1141, Aug. 2011.
- [17] P. A. Shields, M. D. B. Charlton, T. Lee, M. E. Zoorob, D. W. E. Allsopp, and W. N. Wang, "Enhanced light extraction by photonic quasi-crystals in GaN blue LEDs," *IEEE J. Sel. Topics Quantum Electron.*, vol. 15, no. 4, pp. 1269–1274, Jul./Aug. 2009.
- [18] X. H. Li, R. Song, Y. K. Ee, P. Kumnorkaew, J. F. Gilchrist, and N. Tansu, "Light extraction efficiency and radiation patterns of III-Nitride light-emitting diodes with colloidal microlens arrays with various aspect ratios," *IEEE Photon. J.*, vol. 3, no. 3, pp. 489–499, Jun. 2011.
- [19] W. H. Koo, W. Youn, P. Zhu, X. H. Li, N. Tansu, and F. So, "Light extraction of organic light emitting diodes by defective hexagonal-close-packed array," *Adv. Funct. Mater.*, DOI: 10.1002/adfm.201200876, to be published.

- [20] X. Sheng, J. Liu, J. Michel, A. M. Agarwal, and L. C. Kimerling, "Low-cost, deterministic quasi-periodic photonic structures for light trapping in thin film silicon solar cells," in *Proc. 34th IEEE PVSC*, Jun. 2009, pp. 002 395–002 398.
- [21] X. Chen, M. J. Li, J. Koh, A. Artuso, and D. A. Nolan, "Effects of bending on the performance of hole-assisted single polarization fibers," *Opt. Exp.*, vol. 15, no. 17, pp. 10 629–10 636, Aug. 2007.
- [22] R. Paschotta, J. Nilsson, A. C. Tropper, and D. C. Hanna, "Ytterbium doped fiber amplifiers," *IEEE J. Quantum Electron.*, vol. 33, no. 7, pp. 1049–1056, Jul. 1997.
- [23] P. K. Mukhopadhyay, K. Özgören, I. L. Budunoilu, and F. Ö. İlday, "All-fiber low-noise high-power Femtosecond Yb-fiber amplifier system seeded by an all-normal dispersion fiber oscillator," *IEEE J. Sel. Topics Quantum Electron.*, vol. 15, no. 1, pp. 145–151, Jan./Feb. 2009.
- [24] S. Hilaire, D. Pagnoux, P. Roy, and S. Février, "Numerical study of single mode Er-doped microstructured fibers: Influence of geometrical parameters on amplifier performances," *Opt. Exp.*, vol. 14, no. 22, pp. 10 865–10 876, Jul. 2006.
- [25] M. Koshiba and K. Saitoh, "Structural dependance of effective area and mode field diameter for Holey fibers," *Opt. Exp.*, vol. 11, no. 15, pp. 1746–1756, Jul. 2003.